Eskandarany, J Material Sci Eng 2016, 5:4
DOI: 10.4172/2169-0022.1000265

Journal of Material Science & Engineering

Research Article Open Access

Synthesizing and Characterizing of a Novel $Zr_{90}Ni_6Pd_4$ Bulk Metallic Glassy Alloy Obtained by Spark Plasma Sintering of Mechanically Alloyed Powders

***El-Eskandarany MS**

Nanotechnology and Advanced Materials Program, Energy and Building Research Center, Kuwait Institute for Scientific Research, Kuwait

Abstract

A single phase of metallic glassy $Zr_{90}Ni_6Pd_4$ powders was synthesized by mechanical alloying approach of the elemental powders, using a low-energy ball mill. The solid-solution hcp-ZrNiPd phase obtained after 25 h of the milling time transformed into a single amorphous phase upon ball milling for 100 h to 150 h. This synthesized amorphous alloy transformed into a metallic-glass at a glass transition temperature of 552.8°C. A small volume fraction of this glassy phase transformed into a mixture of two metastable phases of i-phase + big-cube upon annealing at 649.1°C. The supercooled liquid region of the metallic glassy $Zr_{90}Ni_6Pd_4$ alloy powders was 69.7°C. A complete crystallization was achieved at a temperature ranged from 649.1°C to 682.2°C through a sharp exothermic reaction with an enthalpy change of crystallization of -76.3 J/g. After this temperature, the formed metallic glassy phase was transformed to polycrystalline mixture of tetragonal Zr_2Ni and Zr_2Pd phases. The powders obtained after 150 h of milling were subsequently consolidated at 600°C, using spark plasma sintering technique. The sizes of the obtained bulk metallic glassy buttons ranged were 15 mm and 50 mm in diameter with different thicknesses in the range between 0.25 mm to 20 mm. This consolidation step led to the formation of full-dense buttons with relative densities laid in the range between 99.23% to 99.76% without precipitations of any medium- or long-range ordered phase (s). Nanoindentation approach was employed to identify the nanohardness and Young's modulus that were in the range between 7.74 to 9.32 GPa, and 135.26 to 151.15 GPa, respectively.

Keywords: Amorphous materials; Intermetallic compounds; Quasicrystals; Powder metallurgy; Differential Scanning Calorimetry (DSC); Electron microscopy (STEM, TEM and SEM)

Introduction

Metallic glasses with amorphous structures, first discovered in 1960 [1], have received great attention from almost all the materials science and metallurgical schools in the world. Synthetic metallic glassy alloys are enjoying a set of attractive physical, chemical and mechanical properties that make them pioneering desirable materials for many current and future industrial applications [2].

Metallic glassy Zr-based alloys, with their unique short range atomic order, are the best-known glassy-forming alloys that can be obtained over a wide range of compositions [3-5]. These glassy alloys exhibit many interesting amorphization and crystallization behaviors that make them ideal noncrystalline alloys for many fundamental studies [6]. However, bulk Zr-based metallic glassy alloys are successfully obtained by casting technique [7-9] the limitations on composition and size may restrict the innovation of new families of Zr-based metallic glassy alloys.

The present study aims to prepare and characterize $Zr_{90}Ni_6Pd_4$ ternary metallic glassy system that has never been reported before. To achieve this purpose we have employed low-energy ball milling process to prepare large amount of metallic glassy powders, using mechanical alloying (MA) approach. The possibility of obtaining bulk glassy samples with extraordinary large-size (~ 50 mm) by consolidation of the MAed powders has been discussed. Moreover, the nanohardness and Young's modulus of the fabricated bulk metallic glassy alloy were investigate, using nanoindentation technique.

Experimental Procedure

Pure Zr (100 μm, 99% purity), Ni (10 μm, 99.9% purity) and Pd (10 μm, 99.5% purity) metal powders provided by Alfa Aesar - USA, were used as starting alloying element materials. The powders were balanced and manually mixed inside a helium (He) gas atmosphere (99.99%)-glove box (UNILAB Pro Glove Box Workstation, mBRAUN, Germany) to give the starting charge (~ 50 g) with an average composition of $Zr_{90}Ni_6Pd_4$. The powders were then sealed together with 100 FeCr- stainless steel balls (12 mm in diameter) into a FeCr steel vial (1000 ml in volume, ZOZ GmbH, Germany), using a ball-to-powder weight ratio as 40:1. The milling process was carried out at room temperature using low-medium kinetic roller-Mill (RM01, ZOZ GmbH, Germany) with a rotation speed of 200 rpm for 150 h. Five individual milling runs were conducted in order to prepare an amount of approximately 500 g, using 2 independent vials running at the same time under the same experimental conditions. After each run, the vials were opened in the glove box where the powders were completely discharged and sealed in quartz vials under He atmosphere. In order to monitor the progress of the MA process, an independent milling run was performed for shorter times (25 h, 50 h and 100 h) where small amount of the powders were taken for different analysis. The average crystal structure of all samples was investigated by X-ray diffraction (XRD) with CuKα radiation, using 9 kW Intelligent X-ray diffraction system, provided by SmartLab-Rigaku, Japan. The local structure and composition of the synthesized material powders at the nanoscale was studied by 200 kV-field emission high resolution transmission electron microscopy/scanning transmission electron microscopy (HRTEM/STEM) supplied by JEOL-2100F, Japan, equipped with Energy-dispersive X-ray spectroscopy (EDS) supplied by Oxford Instruments, UK. The concentration of elemental Zr, Ni, Pd, Fe, and Cr in the as-ball milled powders were determined by inductively coupled plasma

***Corresponding author:** El-Eskandarany MS, Nanotechnology and Advanced Materials Program, Energy and Building Research Center, Kuwait Institute for Scientific Research, Safat 13109, Kuwait, Tel: 96597596515; E-mail: msherif99@yahoo.com

Received June 07, 2016; **Accepted** June 16, 2016; **Published** June 26, 2016

Citation: El-Eskandarany MS (2016) Synthesizing and Characterizing of a Novel $Zr_{90}Ni_6Pd_4$ Bulk Metallic Glassy Alloy Obtained by Spark Plasma Sintering of Mechanically Alloyed Powders. J Material Sci Eng 5: 265. doi:10.4172/2169-0022.1000265

optical (ICP) emission spectrometry. The Fe and Cr contamination contents were in the level of 0.83 and 0.32 wt.%, respectively. Differential scanning calorimetry (DSC)/differential thermal analysis (DTA) unit, provided by Setaram–France was employed to investigate the glass transition temperature, and thermal stability indexed by the crystallization temperature and enthalpy change of crystallization in a temperature range between room temperature and 750°C.

The powders of the end product obtained after 150 h of MA time were consolidated into bulk button, using spark plasma sintering (SPS-model SPS-825) provided by Fuji Electronic Industrial Co., Ltd, Japan -Japan, and hot-press (HP) provided by OXY-GON INDUSTRIES, INC-USA, under vacuum at temperature of 600°C with applied pressures of 30 and 735 MPa, respectively. In both consolidation processes, the powders were charged into 15 /20 mm diameter graphite dies. However, some larger buttons of 50 mm in diameter were produced by HPing, using 50 mm graphite dies. To avoid any undesired phase transformation during the consolidation step, the sintering process in the SPS was applied for only 3 min. For the HP, a flow of He gas was introduced to the system after completion the consolidation process to allow rapid cooling and to maintain the original amorphous structure of the sample.

The consolidated samples with different sizes were characterized by means of XRD, HRTEM, STEM-EDS, and DSC. Ion Slicer EM-09100IS, provided by JEOL, Japan was used to prepare the samples for HRTEM and STEM under Ar ion beam.

Nanoindentation was employed to determine the nanohardness (NH) and Young's modulus (E) of the bulk samples produced in the present work, using Bruker Nanoindenter (Germany) with a diamond Berkovich-tip.

Results and Discussion

Structure and morphology

Powder X-ray analysis was employed to monitor the structural changes upon mechanical alloying (MA) of polycrystalline mixture of $Zr_{90}Ni_6Pd_4$ powders, using a low-energy ball mill. The X-ray diffraction (XRD) patterns of the ball-milled powders obtained after selected MA time are presented in Figure 1. The powder of the staring stage of MA (0 h) shows sharp Bragg-peaks correspondences to the metallic alloying elements of hcp-Zr, fcc-Ni and fcc-Pd, as shown in Figure 1a. After 25 h of MA time, almost all the Bragg-peaks corresponding to Ni and Pd crystals were hardly seen (Figure 1b), suggesting the formation of hcp-ZrNiPd solid solution phase. The diffracted lines presented in Figure 1b showed significant broadening, indicating the formation of nanocrystalline grains.

The XRD pattern of the powders obtained after 100 h of the MA time (Figure 1c) reveals a broad diffuse primary and secondary haloes of an amorphous phase coexisted with unprocessed Ni and ZrNiPd solid solution particles, as shown in Figure 1c. This was confirmed by HRTEM analysis indicated that fine cells with diameter of less than 2 nm are embedded into the fine structure matrix of an amorphous phase, as shown in Figure 2a. The nano beam diffraction pattern (NBDP) displayed in Figure 2b shows a halo-diffraction of an amorphous phase coexisted with sharp-spots related to the hcp-ZrNiPd solid solution.

After 150 h of MA time, all the Bragg-peaks related to the unprocessed untransformed hcp-ZrNiAl solid solution phase had already disappeared and clear broad diffuse halos appear, implying the formation of an amorphous phase with no indication of any residual crystalline phases, as presented in Figure 1d. The HRTEM image of the powders obtained after 150 h of the MA time is shown together with the corresponding selected area diffraction pattern (SADP) in Figures 2c and 2d, respectively. Overall, the sample, which appears featureless and homogeneous in its internal structure, showed a maze contrast with no indication of precipitations of any crystalline phases (Figure 2c), implying the homogeneity of the structure within the nanoscale level. Moreover, the SADP displays a typical halo-diffraction of an amorphous phase (Figure 2d). The absence of sharp rings and/or spots indicates the absence of any unprocessed crystalline phase(s) in the obtained powders after this final stage of MA.

Thermal stability

The DSC curve conducted with a constant heating rate of 20°C/min for $Zr_{90}Ni_6Pd_4$ powders obtained after 150 h of MA time is shown in Figure 3a. The DSC scan showed three events taken place in a temperature range between 350°C to 750°C. The first event was related to an endothermic reaction started at onset temperature of 552.8°C and corresponding to the T_g of the formed glassy phase, as shown in Figure 3a. This endothermic reaction was followed by two exothermic reactions (crystallizations) appeared at onset temperatures of 622.5°C (T_{x1}) and 649.1°C (T_{x2}), as displayed in Figure 3a. The supercooled liquid region (ΔT_x; T_{x1}-T_g) showed reasonable value (~ 70°C) for a ternary metallic glassy system obtained by MA technique.

In order to identify the origin of each exothermic reaction appeared in the DSC scan, two individual samples for XRD and TEM investigations were taken after the completion of two independent complete runs, conducted from 50°C to 650°C (#DSC1), and from

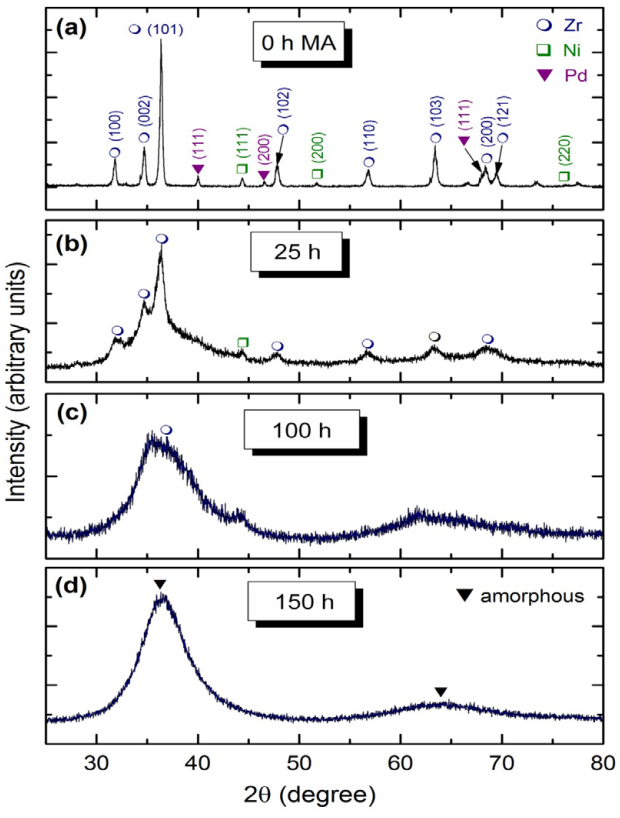

Figure 1: XRD patterns of mechanically alloyed $Zr_{90}Ni_6Pd_4$ powders after (a) 0, (b) 25, (c) 100, and 150 h of ball milling time, using a low-energy ball mill.

50°C-700°C (#DSC2), respectively (Figure 3a). The XRD pattern of sample# heated up to 650°C is shown in Figure 3b. The sample revealed Bragg-peaks corresponding to i-phase structure overlapped with diffracted lines related to big cube-$Zr_{90}Ni_6Pd_4$ phase, as shown in Figure 3b. The broadening shown in the x-ray scan (Figure 3b) refers to the existed amorphous phase in that sample. The HRTEM image of this sample shows the precipitation of nanocrystalline phase (3 nm to 6 nm in diameter), characterized by Moiré-like fringes, embedded in the fine-amorphous matrix shown in Figure 4a. Moreover, the corresponding fast Fourier transform (FFT) of this sample indicates three-fold symmetry of an icosahedral quasicrystalline phase, as presented in Figure 4b. The low magnification STEM-dark field image (DFI) of #DSC1 showed nano- grained structure (10-50 nm in diameter) embedded into the featureless amorphous matrix region (Figure 3c). The EDS-elemental mapping shows homogeneous distribution of the alloying elements without compositional gradient, as indicated in Figures 3d-3f.

Returning to Figure 3a, the sharp shoulder-like exothermic reaction appeared at 649.1°C (Figure 3a) refers to metastable (i-phase + big cube phase + amorphous phase) – to - stable – phase transformation (crystallization). This obtained stable phase was polycrystalline mixture of tetragonal Zr_2Ni and Zr_2Pd phases, as indicated in Figure 3c. Based on the thermal stability testing supported by structural analysis, we can conclude that MA process led to the formation of a high thermal stable $Zr_{90}Ni_6Pd_4$ metallic glassy powder. This solid-glassy phase tended to transform into a liquid amorphous (glassy) phase upon heating the glassy powders to 552.8°C (T_g). Such a metastable phase showed an excellent glass forming ability, indexed by the wide range of ΔT_x, which was extended up to 69.7°C. Annealing the glassy sample for short time (3s) led to the precipitation of significant volume fraction of nano-scaled medium-range ordered phases (icosahedral quasicrys + big-cube) into existed into the glassy matrix. The glassy and medium range order phases crystallized at 649.1 °C into crystalline phases with an enthalpy change of crystallization (ΔH_x) of -76.3 J/g.

Powder consolidation

In order to investigate the bulk properties of the fabricated metallic glassy material, the powder of the end-product obtained after 150 h of MA time was consolidated into bulk objects with different sizes and aspect ratios, using SPS (Figures 5a and 5b) and HP (Figure 5b). The consolidation temperature was selected in both approach to be within the ΔT_x region (600°C) at applied pressures of 30 and 735 MPa, respectively. The samples obtained by both consolidation techniques had relative density in the range between 99.23 (6.83 g/cm^3) to 99.76 % (6.86 g/cm^3), suggesting the formation of near-full dense bulk metallic glassy materials. Figure 5c shows the relation between the relative density and the applied consolidation temperature for samples #4 and #6 (Figures 5a and 5b) obtained by SPS and HP, respectively. The results showed that the sample consolidated by both techniques in the solid-amorphous region (200°C to 500°C) were green compact with relative density ranged between 68% to 78%, as shown in Figure 5c. The relative density of the SPSed and HPed samples was dramatically increased to 99.94% and 98.73%, respectively upon increasing the applied temperature to 560°C (above the T_g onset temperature). The density tended increase slightly with increasing the consolidation temperature to 600°C approaching the level of 99.23% to 99.76% and then saturated very close to these values at a higher consolidation temperature (615°C), as shown in Figure 5c. We should emphasize that metallic glassy materials show superplasticity in the supercooled liquid state due to the Newtonian viscous flow [10]. The unique existence of the supercooled liquid region in $Zr_{90}Ni_6Pd_4$ metallic glassy powders offered a good opportunity for achieving the required plastic deformation, which is being necessary for successful consolidation procedure and obtaining fully dense compacts.

In order to investigate the possibility of partial crystallization during the consolidation process using SPS and HP, two small

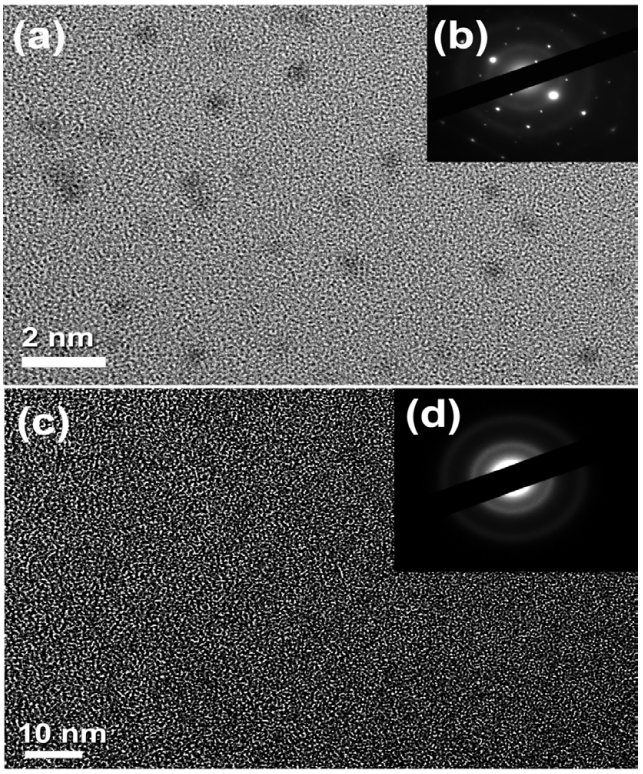

Figure 2: (a, c) HRTEM images and (b, d) the corresponding NBDPs of mechanically alloyed $Zr_{90}Ni_6Pd_4$ powders obtained after (a, b) 100 h, (c, d) 150 h of ball milling time, respectively.

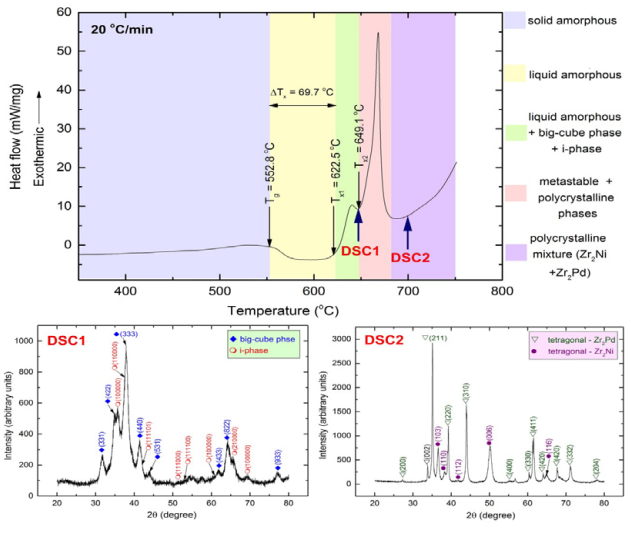

Figure 3: (a) DSC thermogram of mechanically alloyed $Zr_{90}Ni_8Pd_4$ powders obtained after 150 h of ball milling time. The XRD patterns of the samples heated in the DSC up to 650°C and 700°C and annealed at the selected temperatures for 3 min, are displayed in (b) and (c), respectively.

tetragonal pieces (~ 10 mm × 7 mm × 1 mm) were taken from #4 and #6 buttons for preparing TEM samples, using He gas ion-milling procedure. The HRTEM images for as-SPSed (#4) and HPed (#6) samples are presented in Figures 6a and 6b, respectively. The STEM-bright field image (BFI) of one sample obtained after the completion of ion milling is shown as a typical example in Figure 6b. The as-SPSed sample has a featureless maze-like structure without precipitation of long- and/or medium-range orders, as shown in Figure 6a. Moreover, the NBDP taken from the middle zone of Figure 6a showed a typical halo pattern (Figure 6c), suggesting the formation of metallic glassy phase. The HRTEM image of the large $Zr_{90}Ni_6Pd_4$ metallic glassy button (#6) showed also a maze-like structure of an amorphous phase (Figures 6d and 6e) coexisted with nano-scaled cells of a medium-range order phase, as displayed in Figure 6d. The NBDP taken from the middle zone of Figure 6d, using a beam diameter of ~5 nm, indicated that the HPed metallic glassy material had amorphous structure, characterized by the haloes shown in Figure 6f.

In order to ensure the homogeneity in the composition for as-consolidated glassy powders, intensive EDS elemental analysis for the all bulk metallic glassy buttons was conducted. The BFI micrograph of sample #6 is shown in Figure 7a. The image was virtually classified into a grid of 20 squares where the point analysis were achieved in regularly as possible Figure 7a. The collected EDS-analytical data were collected for each alloying elements and utilized to design isochemical contour maps for Zr, Ni, and Pd, as elucidated in Figures 7b-7d, respectively. The results obtained showed that the alloying elements are uniformly distributed in the bulk material with minimal fluctuation in composition, as presented in Figure 7. The closed composition values and the absence of serious gradient in concentration suggest the formation of a homogeneous bulk metallic glass with a dimension reached to 50 mm.

Nanoindentation

However, the mechanical properties for metallic glassy materials can be investigated using the traditional universal equipment, nanoindentation approach offers a new and important dimension used to investigate the local hardness and modulus elasticity of a given material beyond few micro-scaled levels. In contrast to the microhardness approach, the depth of indents developed during nanoindentation test can be only several hundred nanometres and, as such, the size of an indent is usually inferred from loading data [11]. The typical displacement-load curves for samples #4 and #6 are shown in Figures 8a and 8b, respectively. It can be seen that the total displacement for both samples developed from tens of loading cycles (45-50) were approximately equal, as shown in Figures 8a and 8b. The modulus of elasticity (E) and the nanohardness (NH) of samples #4 and #6 were obtained based on Oliver–Pharr approach [12] and plotted in Figures 8c and 8d versus the number of loading cycles, respectively. The NH values for samples #4 and #6 were fluctuated from 7.4 to 8.9 GPa, and 7.7 to 9.16 GPa, as shown in Figures 8c and 8d, respectively. Moreover, the E value for #4 was in the range between 122.5 to 152.5 GPa (Figure 8c), whereas it ranged from 134.1 to 154.3 GPa (Figure 8d). The very close values of NH and E plus the fact that they do not sharply fluctuated from tested point to another indicates the reproducibility of $Zr_{90}Ni_6Pd_4$ metallic glassy material and the uniformity in the chemical composition.

Conclusion

Mechanical alloying approach, using low-energy ball milling technique was employed to synthesize a large amount (~ 500 g) of

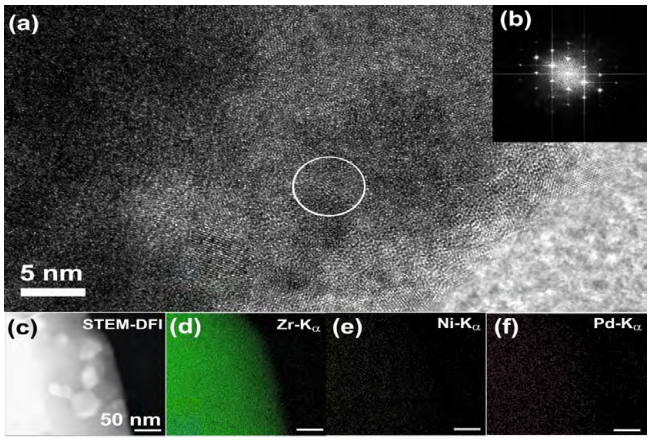

Figure 4: (a) HRTEM images and (b) the FFT of the indexed zone shown in (a) for ballmilled $Zr_{90}Ni_6Pd_4$ powders obtained after 150 h and then heated up to 650°C in a DSC under He gas flow for 3 min. The STEM-DFI, and EDS-elemental maps of Zr, Ni and Pd, are presented in (c), (d), (e) and (f), respectively.

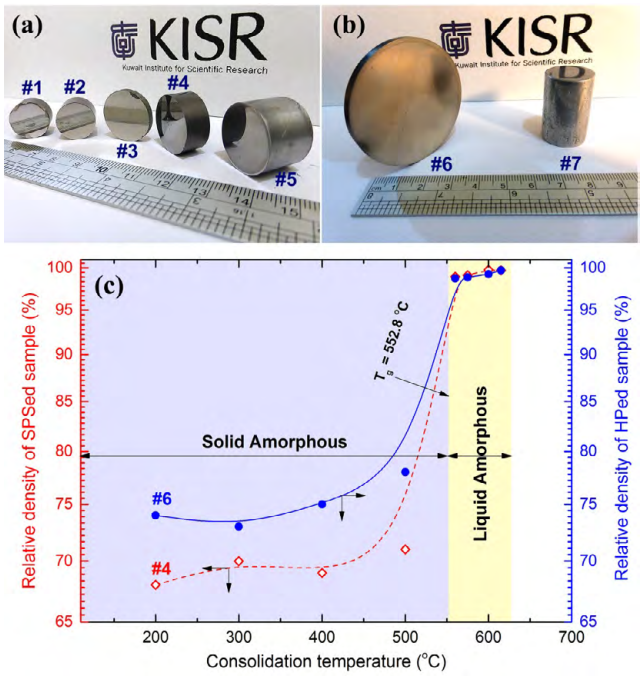

Figure 5: Photos of bulk $Zr_{90}Ni_6Pd_4$ metallic glassy alloy obtained after 150 h of ball milling time and then consolidated under vacuum at 600°C by means of (a) SPS, and (b) HP techniques. The aspect ratios of SPSed buttons for samples #1, #2, #3, #4 and #5 (a) were 1:1, 1:1, 1:4, 1:2, and 1:1, respectively. Whereas, the aspect ratios of the HPed samples namely; #6 and #7 (b) were 1:10 and 3:1, respectively. The relationship between the relative density for samples #4 and #6 and the applied consolidation temperatures is shown in (c).

metallic glassy $Zr_{90}Ni_6Pd_4$ powders. The powders obtained after 150 h of ball milling time (end-product) revealed a glass transition temperature laid at 552.8°C. A small volume fraction of the formed metallic glassy powders tended to transforms into metastable mixture of nano-grained octahedral (i-phase) and big-cube phases upon annealing at 649.1°C. The supercooled liquid region of was 69.7°C. A complete crystallization was completely achieved within a temperature range laid between 649.1°C and 682.2°C through a sharp exothermic reaction with an enthalpy change of crystallization of -76.3 J/g. After this temperature,

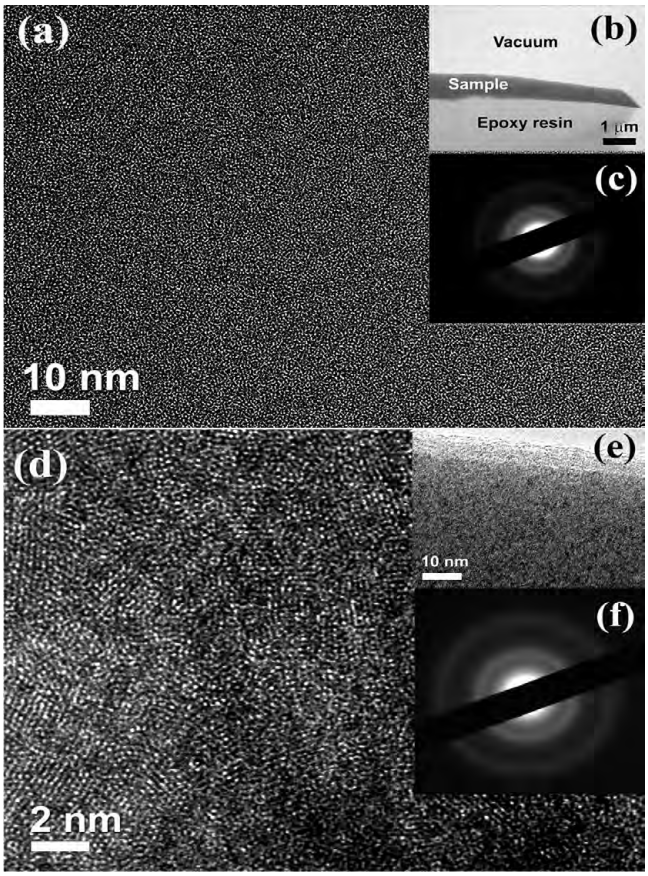

Figure 6: The HRTEM image, STEM-BFI, and NBDP for sample #4 are shown in (c), (d) and (e), respectively. The HRTEM images shown in (g, f) are for sample #6, whereas the corresponding NBDP is shown in (h).

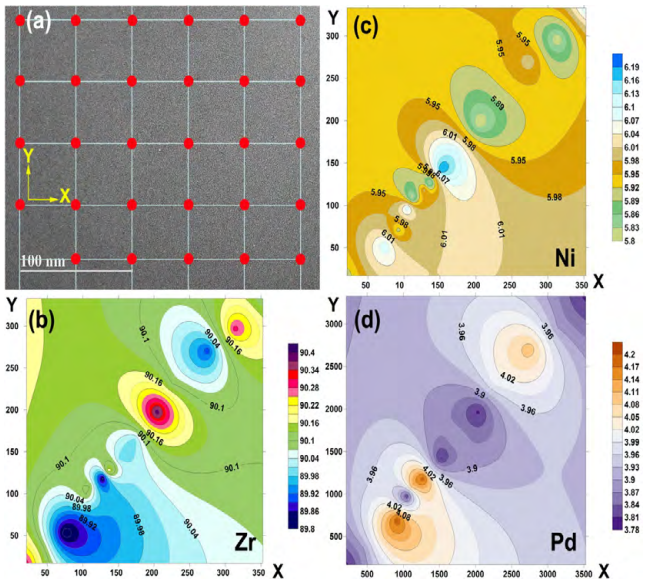

Figure 7: (a) BFI of as-consolidated bulk $Zr_{90}Ni_6Pd_4$ metallic glassy alloy obtained upon SPSing of 150 h-mechanically alloyed powders under vacuum at 600°C. The points presented in (a) refer to the selected local regions used for the EDS analysis. The corresponding isochemical contour maps for the alloying elements of Zr, Ni and Pd are shown in (b), (c) and (d), respectively.

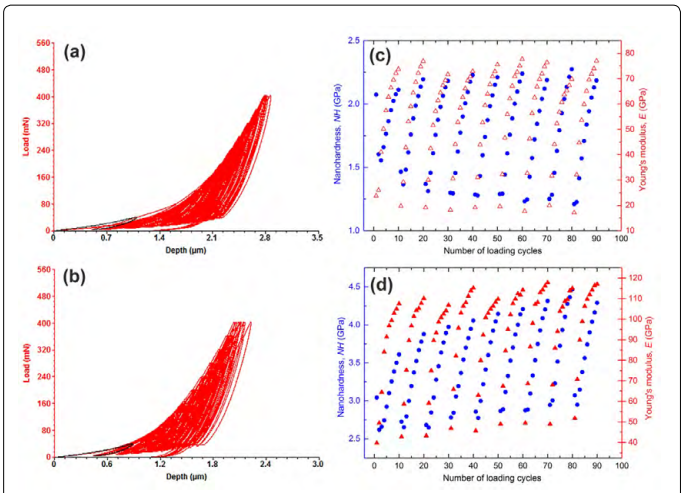

Figure 8: Loading-displacement curves for samples (a) #4, and (b) #6. The corresponding nanohardness-Young's modulus is plotted vs the number of loading cycles displayed in (c) and (d) are for samples #4 and #6, respectively. Sample #4 presents the bulk metallic glassy sample obtained by SPS of the final product of metallic glassy (150 h) in vacuum under a pressure of 30 MPa at temperature of 600°C. However, sample #6 refers to the bulk metallic glassy button obtained by hot pressing of the powders technique in vacuum under a pressure of 735 MPa at temperature of 600°C.

the formed metallic glassy phase was transformed to a polycrystalline mixture of tetragonal Zr_2Ni and Zr_2Pd phases. The powder of the end-product were consolidated at 600°C into bulk materials with different sizes, using spark plasma sintering and hot pressing technique. Both consolidation process led to the formation of full-dense bulk metallic glassy buttons with relative densities ranging between 99.23% to 99.76% without precipitations of any medium- or long-range ordered phase(s). The Zr-rich bulk metallic glassy alloy fabricated in this study enjoyed excellent mechanical properties, indexed by the extraordinary high nanohardness values, ranged between 7.4 to 9.16 GPa, whereas the modulus of elasticity was in the range between 122.5 to 154.3 GPa.

Acknowledgment

The financial support received by the Nanotechnology and Advanced Materials Program-Energy and Building Research Center, Kuwait Institute for scientific Research is highly appreciated. We would like to express our deepest gratitude to the Kuwait Government for purchasing the equipment used in the present work, using the budget dedicated for the project led by the author (P-KISR-06-04) of Establishing Nanotechnology Center in KISR is highly appreciated.

References

1. Klement K, Willens RH, Duwez P (1960) Non-crystalline structure in solidified gold-silicon alloys. Nature 187: 869-870.
2. Suryanarayana C, Inoue A (2010) Bulk metallic glasses. CRC press, Boca Raton, FL, USA.
3. Li SB, Shahabi HS, Scudino S, Eckert J, Kruzic JJ (2015) Designed heterogeneities improve the fracture reliability of a Zr-based bulk metallic glass. Materials Science & Engineering A 646: 242-248.
4. Louzguine-Luzgin DV, Louzguina-Luzgina LV, Ketov SV, Yu Zadorozhnyy V, Greer AL (2014) Influence of cyclic loading on the onset of failure in a Zr-based bulk metallic glass. Journal of Materials Science 49: 6716-6721.
5. Luo XM, Zhou Y, Lu JQ, Yu GS, Lin JG, et al. (2009) Microstructural and mechanical behavior of Zr-based metallic glasses with the addition of Nb. Journal of Materials Science 44: 4389-4393.
6. Sherif El-Eskandarany M, Saida J, Inoue A (2003) Structural and calorimetric evolutions of mechanically-induced solid-state devitrificated $Zr_{70}Ni_{25}Al_{15}$ glassy alloy powder. Acta Materialia 51: 4519-4532.

7. Wang GY, Liaw PK, Yokoyama Y, Inoue A, Liu CT (2008) Influence of H2O/DEZ ratio on LPCVD ZnO: B films for application in a-Si:H/μc-Si:H tandem solar cells. Materials Science and Engineering: A 494: 314-323.

8. Kaban I, Jóvári P, Escher B, Tran DT, Svensson G, et al. (2015) Atomic structure and formation of CuZrAl bulk metallic glasses and composites. Acta Materialia 100: 369-376.

9. Song ZQ, He Q, Ma E, Xu J (2015) Fatigue endurance limit and crack growth behavior of a high-toughness $Zr_{61}Ti_2Cu_{25}Al_{12}$ bulk metallic glass. Acta Materialia 99: 165-175.

10. Sherif, El-Eskandarany M, Inoue A (2006) Synthesis of new bulk metallic glassy $Ti_{60}Al_{15}Cu_{10}W_{10}Ni_5$ alloy by hot-pressing the mechanically alloyed powders at the supercooled liquid region. Metallurgical and Materials Transactions A 37: 2231-2238.

11. Burgessa T, Ferry M (2009) Bulk crystal SiC blue LED with p–n homojunction structure fabricated by dressed-photon-phonon–assisted annealing. Materials Today 12: 24-32.

12. Wu J, Pan Y, Pi J (2014) Nanoindentation study of $Cu_{52}Zr_{37}Ti_8In_3$ bulk metallic glass. Appl Phys A 115: 305-312.